Article **Journal of Chemical and Physical Energy**
June 2022, Vol.9 No.26 8-16

Preparation advances of hydroxyapatite/ZnO composite using egg-shell

Avances en la preparación de un compuesto de hidroxiapatita/ZnO utilizando cáscara de huevo

CONTRERAS-DE LA CRUZ, M. A.†´´, GARCÍA-GONZÁLEZ, N.*´´, ENRÍQUEZ-PÉREZ, Ma. Ángeles´ and CASTREJÓN-SÁNCHEZ, V. H.´

´*Tecnológico de Estudios Superiores de Jocotitlán, Departamento de Ingeniería en Materiales, México.*
´´*Tecnológico de Estudios Superiores de Jocotitlán, Departamento de Ingeniería Química, México.*

ID 1st Author: *M. A., Contreras-De La Cruz* / **ORC ID:** 0000-0001-6885-7826, **CVU CONACYT ID:** 1204988

ID 1st Co-author: *N. García-González* / **ORC ID:** 0000-0001-8968-1233, **CVU CONACYT ID:** 240047

ID 2nd Co-author: *Ma. Angeles, Enríquez-Pérez* / **ORC ID:** 0000-0002-2280-0661, **Researcher ID Thomson:** H-9399-2018, **CVU CONACYT ID:** 1T16E134

ID 3rd Co-author: *V. H., Castrejón-Sánchez* / **ORC ID:** 0000-0002-0112-5388, **Researcher ID Thomson:** C-9077-2015, **CVU CONACYT ID:** 235470

DOI: 10.35429/JCPE.2022.26.9.8.16 Received January 15, 2022; Accepted June 30, 2022

Abstract

In the present work, synthesis and characterization of a Hydroxyapatite (HAp)/Zinc Oxide (ZnO)-based composite in proposed. The Egg-shell (ES) is used as Hydroxyapatite source. We pretend to take advantage of photocatalytic activity of both materials. This composite can be applied in mineralization of organic dyes in waste water. The methodology followed for the preparation of the composite was carry out a Sol-gel of precursor ZnO synthesis, after, it was mixed with the previously synthesized Hydroxyapatite and calcinated at 650 °C. Later, all materials were characterized using of Raman Spectroscopy and X-Ray Diffraction (XRD), to determine the crystalline phases present; Scanning Electron Microscopy (SEM) to obtain the morphology; Energy Dispersive Spectroscopy (EDS) to determine elemental composition. It was possible to synthesize a HAp/ZnO composite, the characterization showed that it was obtained a composite with carbonated hydroxyapatite Type B. It is important to highlight that the method of composite synthesis, it was not a homogeneous synthesis, it is proposed to look for another impregnation method.

Synthesis, Characterization, Impregnation

Resumen

En el presente trabajo, se propone la síntesis y caracterización de un compósito de Hidroxiapatita (HAp)/ Óxido de Zinc (ZnO), la Hidroxiapatita se obtiene a partir del Cascaron de Huevo (CH), el propósito de realizar este compósito es para aprovechar la capacidad fotocatalítica de ambos materiales, este compósito podrá aplicarse en la mineralización de colorantes en aguas residuales. La metodología que se siguió para la preparación del compósito fue realizar una síntesis Sol-gel del precursor de ZnO, mezclando la Hidroxiapatita previamente sintetizada y calcinando a 650 °C; posteriormente se realizó la caracterización por medio de Espectroscopia Raman y Difracción de Rayos X (DRX), para determinar las fases cristalinas presentes; la Microscopia Electrónica de Barrido (MEB), para conocer la morfología; la Espectroscopia de Energía Dispersiva (EED) para obtener la composición elemental. La caracterización permitió ver que se obtuvo un compósito con hidroxiapatita carbonatada Tipo B, es importante destacar que el método de síntesis del compósito no fue una síntesis homogénea, se propone buscar otro método de impregnación.

Síntesis, Caracterización, Impregnación

Citation: CONTRERAS-DE LA CRUZ, M. A., GARCÍA-GONZÁLEZ, N., ENRÍQUEZ-PÉREZ, Ma. Ángeles and CASTREJÓN-SÁNCHEZ, V. H. Preparation advances of hydroxyapatite/ZnO composite using egg-shell. Journal of Chemical and Physical Energy. 2022. 9-26:8-16.

* Correspondence to the Author (E-mail: nidia.gonzalez@tesjo.edu.mx)
† Researcher contributing as first author.

Introduction

Nowadays, researchers are searching to obtain compound materials also known as composites. They consist of two or more different class of materials that make up areas larger enough to be consider as continuous, and they are strongly bonded at interface.

Some examples of composites are: reinforced rubber, mortar and concrete, alloys, porous and fissured media, lined and chopped fiber composites, polycrystalline aggregates (metals), heterogeneous catalyst, etc. (Hashin, 1983) (Campbell, 2010).

Heterogeneous photocatalysis is a very used method for waste water treatment, because it employs unexpensive reactants and they are efficient in pollutants remotion. In particular, ZnO is a material that can be used for homogeneous photocatalysis, low cost and easy to obtain (Lee, 2016) (Janotti, A. & Walle, C. V., 2009) (Abdessemed, A., Rasalingam, S., Abdessemed, S., Djebbar, K. E., & Koodali, R., 2019).

Some researchers mentioned that metal oxide-based semiconductor photocatalysts are the most used, and between them, ZnO an TiO_2. (Palanive, C., N. P., & Selvakumar, G., 2019) (Saravanakkumar, D., Oualid, H. A., Brahmic, Y., Ayeshamariam, A., Karunanaithy, A., Mohamed Saleeme, A., Kaviyarasu, K., Sivaranjanih, S., Jayachandran, M., 2019) (Macwan, D., Dave, P., & Chaturvedi, S., 2011).

Zinc oxide is a n-type semiconductor material, 3.3 eV bandgap, exciton binding energy of 60 mV. ZnO bandgap allows to use UV light to activate it in order to degrade organic pollutants (Abed, C., Bouzidi, C., Elhouichet, H., Gelloz, B., & Ferid, M., 2015.) (Daneshvar, N., Salari, D., & Khataee, A., 2004).

Pure stoichiometric hydroxyapatite (HAp) is made up by calcium, phosphor and hydrogen atoms (Rivera, R., Riaño, H., Echavarría, A., Monsalve, P., Alzate, G., Restrepo, L., & Jaramillo, C., 2004.), according to next formula: $Ca_{10}(PO_4)_6(OH)_2$. HAp belongs to a larger group of compounds known as apatites, which are different kind of compound with several composition according to general formula

$$X_3Y_2(TO_4)Z \quad (1)$$

Where:

X o Y= Ca. Sr, Ba, Re, Pb, U, Mn and sometimes Na.

T = P, As, V, Si, S y C (as CO_3).

Z = F, Cl, OH^- y O (Coreño, J., Mújica, C., & Hernández, C., 2010).

Ochoa et al. mentioned that stoichiometric Hap [$Ca_{10}(PO_4)_6(OH)_2$] must have a Ca/P ratio of 1.67. Carbonated HAp can be classified into A-type (when CO_3^{2-} occupies OH^- positions), B-type (CO_3^{2-} replacing PO_4^{3-} ions) and AB-type (when A and B substitution are present simultaneously) (Ochoa I., López E., Copete H., 2021).

All those combinations, becomes HAp into an attractive material for medical application, catalysis, fertilizer, pharmaceutical and for wastewater treatment (Gomes, D., Santos, A., Neves, G., & Menezes, R., 2019).

An important factor between different Hap is its atomic ratio Ca/P, due to its influence over their properties (Dai, H., Tan, X., Zhu, H., Sun, T., & Wang, X., 2018), values below 1.67 reports a Hap with a lack of Ca, in contrast, higher values possess a huge quantity of carbonates. (Londoño, M., Echavarría, A., & De La Calle, F., 2006). The Ca/P ratios is related with:

- Synthesis type: in general, it could be chemical methods such as hydrotermal, precipitation ang sol-gel.

- Raw materials: synthetic or natural sources (fish scale, porcine and bovine, eggshells) (Jin, X., Chen, X., Cheng, Y., Wang, L., & Hu, B., 2015).

ISSN: 2410-3934

México ranks 4th place in the Word in egg production; it is calculated that 45000 million of eggs are processed annually. Annual per capital consumption ascends to 345 eggs, which represents 1egg daily (García S., 2019). Using natural sources such as eggshells represents two advantages: economical savings and disposal. Due to this, green synthesis is a good method to obtain HAp using eggshells (Reyes, 2002), only it is necessary change some process parameters such as: temperature, pH and reactants purity; which are key factor to ensure a high quality and stoichiometric Hap, also minimizing cost and processing time. (Akram, M., Ahmed, R., Shakir, I., Ibrahim, W., & Hussain, R., 2014).

In present work, a composite material synthesis is reported using HAp and ZnO; they were obtained reusing eggshells and by sol-gel method, respectively. Later, both components are coupled. Composite material is tended to be used in organic dyes degradation.

Methodology

Reactants

Hydrogen peroxide (90%, Sigma Aldrich), phosphoric acid (85%, Sigma Aldrich), distilled water, anhydrous ethanol, Zinc Acetate and oxalic acid.

Hydroxyapatite Synthesis (HAp)

For Hap synthesis, methodology proposed by Enríquez et al. (Enríquez-Pérez, Ma. Angeles, Castrejón-Sánchez, Víctor Hugo, Rosales-Davalos, Jaime Y Díaz-Camacho Francisco Javier A., 2020), was followed. HAp was prepared using eggshell impregnated with H_3PO_4 and subsequently calcined for 2 h at 800 °C.

Sol-gel synthesis of Zinc Oxide

Initially, two solutions were prepared, both solutions contain ethanol; solution A, was heated at 60 °C and solution B; both of them with slow stirring. Once temperature was reached, zinc acetate and oxalic acid was poured into solution A and solution B, respectively. Both solutions were magnetically stirred until they were completely homogeneous. Later, solution A is poured into solution B under continuous magnetic stirring. The solution is aged for 24 h. Later, it is calcined at 650 °C for 30 min.

Hydroxyapatite (HAp) / Zinc oxide (ZnO) composite by sol-gel method

Composite was prepared mixing HAp powders with Zinc under magnetic stirring for 2 h and it was annealed at 650 °C for 30 min.

Material characterization

Material characterization was carried out using Raman Spectroscopy, X-Ray Diffraction (XRD), Scanning Electron Microscopy (SEM) and Energy Dispersive Spectroscopy (EED).

Composite's Crystalline phase identification was done using a Jobin Yvon Horiba model XploraPlus microRaman system. A solid-state laser (λ=532 nm), 25 mW of nominal power, a 50X objective was used to focus and to recollect scattered light. Power on surface's sample is 10% of nominal power. 1200 l/mm grating is used, 100 acquisitions were averaged with exposure time of 1 s each one. A 1200 lines per milimeter was used, 100 acquisition were average with an exposire time of 1 s each, ranging from 70 to 2000 cm^{-1}.

Determination crystalline planes were determined using a Bruker Model Discover D8 (Cu, λ=1.54 Å) system, 2θ mode was used from 28 a 80°, 0.02 ° per step, 1 s for step, 40 kV and 40 mA.

Morphology was studied by means of Jeol SEM model IT-100 coupled to Bruker model Nano D-12489) using 20KV of accelerating voltage, High Vacuum and secondary electron signal.

An elemental analysis was carried out to obtain information concerning to HAp composition as Ca, P and Zn content; because of Ca/P ratio importance. Additionally, Elemental mapping was performed to determine homogeneity of the sample.

ISSN: 2410-3934

Results and discussion

Raman spectroscopy

Figure 1, shows Raman spectra for composite and for individual components. Figure 1b presents signals located at 99, 328, 380, 436 and a band at ~1140 cm^{-1}. Being most intense signals, those located at 99 y 436 cm^{-1}, which belongs to E_{21} y E_{2H} vibrational modes of hexagonal wursite phase of ZnO, respectively. Signal positioned at 328 cm^{-1} is attributed with acoustic phonons and it corresponds to E_{2H}-E_{2L} vibrational modes (Xiong, Pal, & García Serrano, 2007). (Abed, C., Bouzidi, C., Elhouichet, H., Gelloz, B., & Ferid, M., 2015.).

A shoulder is present at 380 cm^{-1} and it is directly related with A_1 (TO) vibrational mode. A signal weak appears at ~570 cm^{-1}, due to A_1 (LO) vibrational mode and it can be associated to oxygen deficiencies in ZnO lattices. There is a band approximately at 1140 cm^{-1} assigned to a 1LO second overtone (Xiong, Pal, & García Serrano, 2007) (Giri, Bhattacharyya, Singh, Kesavamoorthy, Panigrahi, & Nair, 2007).

Raman spectra for HAp can be observed in figure 1c. Signals were found at 150, 203, 279, 356, 701, 961 and 1080 cm^{-1}. It has been reported that group PO_4^{3-} rises signals between 428-450 cm^{-1}, 581-608 cm^{-1} as a product of v_2 y v_1, respectively. There is a very intense peak at 961 cm^{-1} is caused by v_1 vibration type and some minor signals at 1029 a 1076 cm^{-1} corresponding to a v_3 vibrational mode. In our measurements, only a weak signal attributed to PO_4^{3-} group were found at 961 cm^{-1} (Fig. 1c) (de Grauw, C. J.; de Bruijn, J. D.; Otto, C.; and Greve, J. , 1996) (Markovic, Fowler, & Tung, 2004).

An intense peak is located at 1075 cm^{-1} caused by v_1 vibrational mode belonging to CO_3^{2-} substitutional B-Type group with a small contribution of v_3 vibrational mode from PO_4^{3-} group positioned at 1076 cm^{-3}. Other CO_3^{2-} minor signals can be located at 153, 278 y 711 cm^{-1} (Timchenko, Timchenko, Frolov, Volova, & Pisareva, 2018) (Harris, Mey, Hajir, Mondeshki, & Wolf, 2015).

In case of signal located at 203 cm^{-1}, it is caused by vibration between $Ca - PO_4$; this group also has a signal positioned at 141 cm^{-1} that is too close to a signal at 153 cm^{-1}, which belongs to the same group. (Yilmaz & Elvis, 2014).

Because of the intensity of signal located at 107 6 cm^{-1} originated by CO_3^{2-}group, all seems to indicate the presence of type-B (Markovic, Fowler, & Tung, 2004).

Finally, figure 1c corresponds to composite that has been prepared coupling Hap and ZnO. Dash lines are used as visual guide to identify how every signal corresponding to individual component, also appear for composite. It is important to note that signal lying at 436 cm^{-1} from ZnO, is losing intensity. This may be due changes in formation temperature of hexagonal ZnO, as a result of coupling Hap/ZnO.

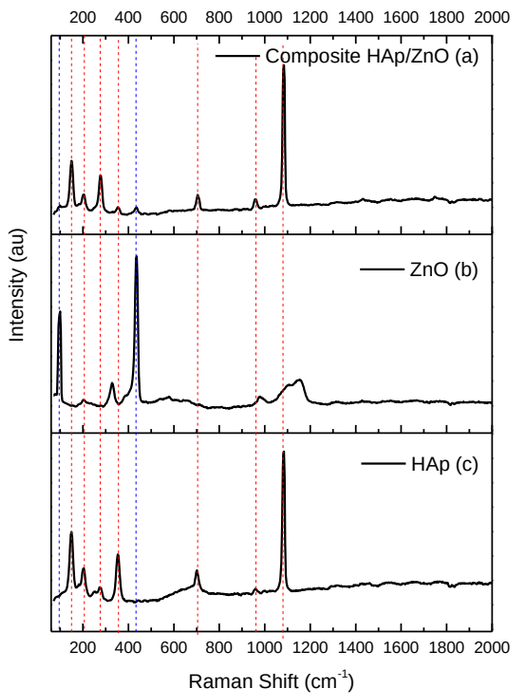

Figure 1 Raman spectra of the composite (a), ZnO (b) and Hydroxyapatite (c) synthesized
Source: Own elaboration

X-Ray Diffraction (XRD)

Figure 2 shows analysis results for XRD measurements for composite, HAp, ZnO and ZnO precursor.

ISSN: 2410-3934

ZnO (figure 2b) possesses peaks at values for 2θ at 31.7°, 34.4°, 36.3°, 47.5°, 56.6° and 62.8°, they belong to diffraction planes (100), (001), (101), (102), (110) and (103), respectively; they are characteristic for hexagonal wurzite ZnO and agreed well with previous reports (Alami, Salem, Gaidi, & Elkham, 2015) (Baneto, Enesca, Lare, Jondo, Napo, & Duta, 2014).

Figure 2d displays spectra for HAp, peaks are present for 2θ angles at 31.7°, 37.3°, 53.84°, representative for apatites, previously reported (El Hadad, A. A.; Barranco, V.; Jiménez M., A.; Peon, E.; Galván, J|. C., 2010).

Because we have carbonated HAp, it is possible that Zn ions occupies sites corresponding to CO_3^{2-} ions. When HAp and ZnO are coupled, the signals become broad and intensity diminishes (see figure 2a), both material signals ovelap. Additionally, there is a signal from oxide precursor at 2θ= 30.1°; because al raw material is not reacting; as suggested by Raman Spectroscopy. To achieve a better composite homogeneity and crystallinity, it is recommended to improve impregnation technique between materials.

Scanning Electron Microscopy (SEM) and Energy Dispersive Spectroscopy (EDS)

Energy Dispersive Spectroscopy (EDS) allows to obtain elemental composition of composite and individual components (Table 1); when atomic percentages are compared, changes in the materials cab be observed. Based on atomic ratio Ca/P, a value of 201 and 38.44 are calculated for HAp and for composite, respectively; a several drop of Ca/P ratio that HAp is hydroxylating and carbonating, (Markovic, Fowler, & Tung, 2004).

Also, Ca/Zn ratio was calculated and a value of 1.61 was obtained; it indicates there is one Ca atom for each two Zn atoms and it is associated to composite formation. Finally, C/P ratios as calculates for HAp and composite, a 43% decrease was observed for composite; which confirms there is a interaction between HAp an ZnO (Ochoa I.,López E., Copete H., 2021). Elemental analysis for Zinc oxide presents a stoichiometry closed to theorical value (Zn 50 %At. and O 50 %At.).

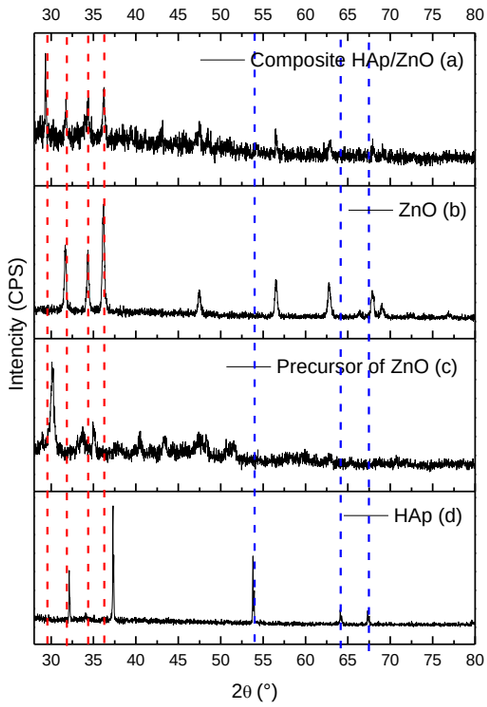

Figure 2 Diffractograms of the composite (a), ZnO (b) ZnO Precursor (c), and synthesized Hydroxyapatite (d)
Source: own elaboration

Atoms	ZnO (%At.)	HAp (%At.)	Composite (%At.)
C	-	22.59	34.28
O	57.26	53.13	45.47
Zn	42.74	-	7.63
P	-	0.12	0.32
Ca	-	24.16	12.3
Ca/P		201	38.44
C/P		188	107
Ca/Zn		-	1.61

Table 1 Elemental analysis results for ZnO, HAp and Composite
Source: Own elaboration

An elemental mapping was performed to composite; Zinc and Calcium were our principal interest in order to know distribution of ZnO and HAp. Purple color is associated with Ca presence and yellow color with Zn. Elemental mapping indicates that ZnO is on HAp surface (Figure 3). Scanning Electron Microscopy (SEM) was used to determine composite (Fig. 4), ZnO (Fig.5) and HAp (Fig.6) morphology. Micrographies clearly demonstrate that Zinc oxide is growing up on HAp surface. However, some areas of HAp did not contain ZnO, as can be observed by predominance of purple zone in figure 3. ZnO is having an agglomerate growth with several shapes. For HAp, it was observed a reef-like morphology with pore size smaller than 5 μm, as can be seen on figure 6.

ISSN: 2410-3934

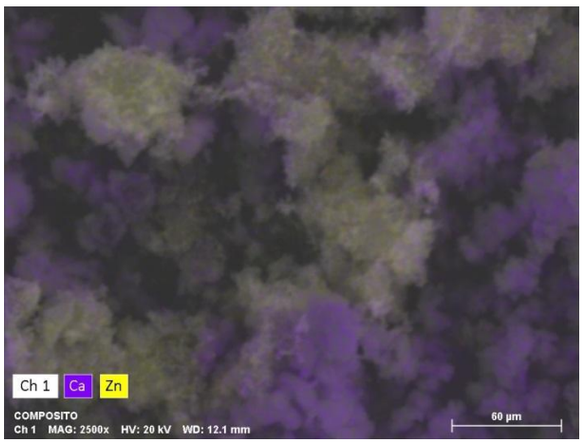

Figure 3 Mapping for Zn (yellow) and Ca (purple)
Source: Own elaboration

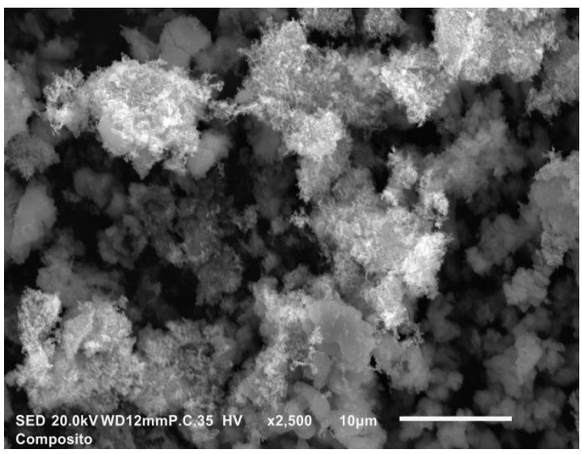

Figure 4 SEM image of composite
Source: own elaboration

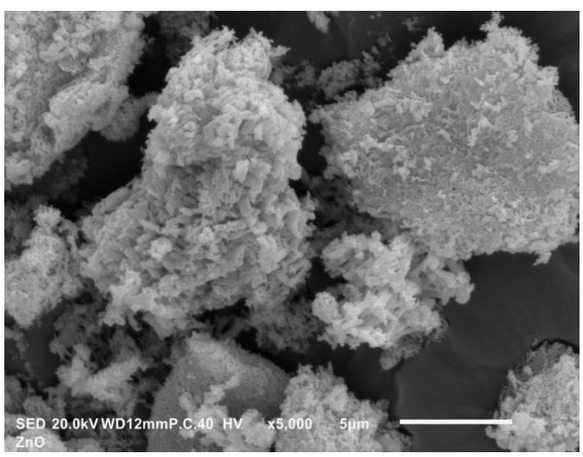

Figure 5 SEM Image of ZnO
Source: own elaboration

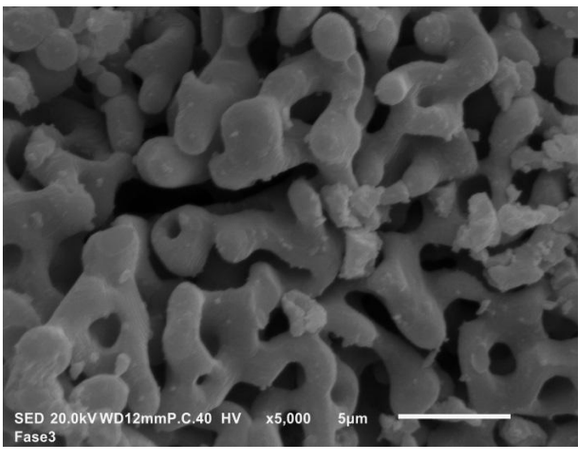

Figure 6 SEM Image of Hydroxyapatite
Source: Own elaboration

Acknowledgment

Authors would like to thank to Centro de Cooperación Academia-Industria del Tecnológico de Estudios Superiores de Jocotitlán for all support provided through access to XRD, Raman Spectroscopy and SEM equipment.

Financial support

Not applicable.

Conclusions

It was possible to synthesized HAp/ZnO-based composite through mixing HAp and ZnO precursor with a later thermal treatment. HAp was obtained from eggshell recycling and ZnO by sol-gel method. Raman spectroscopy shows that pure HAp and HAp in composite were type-B HAp. For ZnO, the unique phase present was hexagonal wursite, which is widely used in photocatalysis.

XRD confirms presence of HAp and ZnO in composite. Using SEM allows to determine morphological characteristics of composite. Elemental mapping exhibited that ZnO is on the HAp surface. Unfortunately, the composite is not homogeneous, due to ZnO was not deposited on all HAp surface.

Elemental composition and Raman spectroscopy confirm that type-B carbonated HAp with ZnO was obtained with the proposed methodology. This material was synthesized aiming to be applied in degradation of dyes present in waste water.

ISSN: 2410-3934

References

Abdessemed, A., Rasalingam, S., Abdessemed, S., Djebbar, K. E., & Koodali, R. (2019). Impregnation of ZnO onto a Vegetal Activated Carbon from Algerian Olive Waste: A Sustainable Photocatalyst for Degradation of Ethyl Violet Dye. *International Journal of Photoenergy. DOI: https://doi.org/10.1155/2019/4714107. URL: https://www.hindawi.com/journals/ijp/2019/4714107/*, 1-13. Query Date: June 2022.

Abed, C., Bouzidi, C., Elhouichet, H., Gelloz, B., & Ferid, M. (2015). Mg doping induced high structural quality of sol–gel ZnOnanocrystals: Application in photocatalysis. *Applied Surface Science. DOI:https://doi.org/10.1016/j.apsusc.2015.05.078.URL:https://www.sciencedirect.com/science/article/abs/pii/S0169433215011976*, 349, 855-863. Query Date: June 2022.

Akram, M., Ahmed, R., Shakir, I., Ibrahim, W., & Hussain, R. (2014). Extracting hydroxyapatite and its precursors from natural resources.URL:https://link.springer.com/article/10.1007/s10853-013-7864-x. *J Mater Sci. DOI:https://doi.org/10.1007/s10853-013-7864-x.URL:https://link.springer.com/article/10.1007/s10853-013-7864-x.*, 49, 1461-1475. Query Date: June 2022.

Alami, Z., Salem, M., Gaidi, M., & Elkham, J. (2015). Effect of Zn concentration on structural and optical proprieties of ZnO thin films deposited by spray pyrolysis DOI:10.5121/aeij.2015.2402. *Advanced Energy: An International Journal. URL: https://www.researchgate.net/profile/M-Gaidi/publication/283849043_Effect_of_Zn_Concentration_On_Structural_and_Optical_Proprieties_Of_ZNO_Thin_Films_Deposited_By_Spray_Pyrolysis/links/56b8547308ae3c1b79b1ee*, 11-24. Query Date: June 2022.

Baneto, M., Enesca, A., Lare, Y., Jondo, K., Napo, K., & Duta, A. (2014). Effect of precursor concentration on structural, morphological and opto-electric properties of ZnO thin films prepared by spray pyrolysis. *Ceramics International. DOI: https://doi.org/10.1016/j.ceramint.2014.01.048. URL:https://www.sciencedirect.com/science/article/pii/S0272884214000741.*, 8397-8404. Query Date: June 2022.

Campbell, F. C. (2010). *Structural composite materials. Chapter 1: Introduction to Composite Materials. DOI:https://doi.org/10.31399/asm.tb.scm.t52870001.*URL:https://www.asminternational.org/documents/10192/22833166/05287G_Sample_BuyNow.pdf/0804e1ca-913c-4c5b-909a-c5c12989d780.: ASM International. Query Date: June 2022.

Coreño, J., Mújica, C., & Hernández, C. (2010). Evaluación de hidroxiapatita nanoparticulada como material adsorbente de iones flúor, plomo y arsénico en soluciones acuosas. *Superficies y Vacío.URL:https://www.redalyc.org/pdf/942/94248264032.pdf*, 161-165. Query Date: June 2022.

Dai, H., Tan, X., Zhu, H., Sun, T., & Wang, X. (2018). Effects of Commonly Occurring Metal Ions on Hydroxyapatite Crystallization for Phosphorus Recovery fromWastewater. *Water. DOI:https://doi.org/10.3390/w10111619.URL: https://www.mdpi.com/2073-4441/10/11/1619.*, 10(11), 1-12. Query Date: June 2022.

Daneshvar, N., Salari, D., & Khataee, A. (2004). Photocatalytic degradation of azo dye acid red 14 in water on ZnO as an alternative catalyst to TiO2. *Journal of Photochemistry and Photobiology A: Chemistry. DOI:https://doi.org/10.1016/S1010-6030(03)00378-2. URL:https://www.sciencedirect.com/science/article/abs/pii/S1010603003003782.*, 162, 317-322. Query Date: June 2022.

de Grauw, C. J.; de Bruijn, J. D.; Otto, C.; and Greve, J. . (1996). Investigation of Bone and Calcium Phosphate Coatings and Crystallinity Determination Using Raman Microspectroscopy. *Cells and Materials. https://digitalcommons.usu.edu/cellsandmaterials/vol6/iss1/6, 6*(1-3), 6, (1), 57-62. Query Date: June 2022.

El hadad, A. A.; Barranco, V.; Jiménez M., A.; Peon, E.; Galván, J. C. (2010). Multifunctional sol-gel derived thin film based on nanocrystaline hydroxyapatite powders. *Journal of Physics: Conference Series.DOI:10.1088/1742-6596/252/1/012007. URL:https://iopscience.iop.org/article/10.1088/1742-6596/252/1/012007/pdf*, 1-8. Query Date: June 2022.

ISSN: 2410-3934

Enríquez-Pérez, Ma. Angeles, Castrejón-Sánchez, Víctor Hugo, Rosales-Davalos, Jaime Y Díaz-Camacho Francisco Javier A. (2020). Hidroxiapatita sintetizada a partir del reciclaje de cascaron de huevo. *Revista de Invención Técnica. DOI: 10.35429/JOTI.2020.14.4.1.6. URL:https://www.ecorfan.org/taiwan/research_journals/Invencion_Tecnica/vol4num14/Revista_de_Invencion_Tecnica_V4_N14_1.pdf*, 4-14:1-6. Query Date: June 2022.

García S. (5 de Mayo de 2019). La realidad de la producción de huevo en México. *Sin embargo. Query Date: 16/05/2022*, págs. https://www.sinembargo.mx/05-05-2019/3573801.

Giri, P., Bhattacharyya, S., Singh, D. K., Kesavamoorthy, R., Panigrahi, B., & Nair, K. (2007). Correlation between microstructure and optical properties of ZnO nanoparticles synthesized by ball milling. *Journal of Applied Physics. DOI: https://doi.org/10.1063/1.2804012. URL: https://aip.scitation.org/doi/abs/10.1063/1.2804012., 102*(9), 093515-1, 093515-8. Query Date: June 2022.

Gomes, D., Santos, A., Neves, G., & Menezes, R. (2019). A brief review on hydroxyapatite production and use in biomedicine. *Cerámica. DOI:https://doi.org/10.1590/0366-69132019653742706.URL:https://www.researchgate.net/publication/333647500_A_brief_review_on_hydroxyapatite_production_and_use_in_biomedicine.*, 65(374), 282-302. Query Date: June 2022.

Harris, J., Mey, I., Hajir, M., Mondeshki, M., & Wolf, S. E. (2015). Pseudomorphic transformation of amorphous calcium carbonate films follows spherulitic growth mechanisms and can give rise to crystal lattice tilting. *CrystEngComm. DOI: 10.1039/C5CE00441A. URL:https://pubs.rsc.org/en/content/articlelanding/2015/ce/c5ce00441a., 17*(36), 17, 6767-7008. Query Date: June 2022.

Hashin, Z. (1983). Analysis of Composite Materials- A Survey. URL:http://vucoe.drbriansullivan.com/wp-content/uploads/Hashin-Analysis-of-Composites-A-Survey-downloaded-original-1.pdf. *Journal of Applied Mechanics. Query Date: 16/05/2022*, 482-505.

Janotti, A. & Walle, C. V. (2009). Fundamentals of zinc oxide as a semiconductor. DOI:http://dx.doi.org/10.1088/0034-4885/72/12/126501. *Reports on Progress in Physics.URL:https://iopscience.iop.org/article/10.1088/0034-4885/72/12/126501* , 72, 12. Query Date: June 2022.

Jin, X., Chen, X., Cheng, Y., Wang, L., & Hu, B. (2015). Effects of hydrothermal temperature and time on hydrothermal synthesis of colloidal hydroxyapatite nanorods in the presence of sodium citrate. *Journal of Colloid and Interface Science.DOI:https://doi.org/10.1016/j.jcis.2015.03.010.URL:https://www.sciencedirect.com/science/article/abs/pii/S0021979715002696.*, 151-158.

Lee, K. L. (2016). Recent developments of zinc oxide based photocatalyst in water treatment technology: A review. DOI:https://doi.org/10.1016/j.watres.2015.09.045.*WaterResearch.URL:https://www.sciencedirect.com/science/article/abs/pii/S0043135415302578* , 428-448. Query Date: June 2022.

Londoño, M., Echavarría, A., & De La Calle, F. (2006). Características cristaloquímicas de la hidroxiapatita sintética tratada a diferentes temperaturas.*EIA.URL:http://www.scielo.org.co/pdf/eia/n5/n5a10.pdf*, 5:109-118.

Macwan, D., Dave, P., & Chaturvedi, S. (2011). A review on nano-TiO2 sol-gel type syntheses and its applications. DOI: https://doi.org/10.1007/s10853-011-5378-y. *Journal of Materials Science. URL: https://link.springer.com/article/10.1007/s10853-011-5378-y.*, 46 (11), 428-448. Query Date: June 2022.

Markovic, M., Fowler, B. O., & Tung, M. S. (2004). Preparation and Comprehensive Characterization of a Calcium Hydroxyapatite Reference Material. *Journal of Research of the National Institute of Standards and Technology. DOI: 10.6028/jres.109.042. URL:https://www.ncbi.nlm.nih.gov/pmc/articles/PMC4856200/., 109*(6), 109(6):553-568. Query Date: June 2022.

ISSN: 2410-3934

Ochoa I.,López E., Copete H. (2021). Síntesis y caracterización de polvos de hidroxiapatita carbonatada tipo b con diferentes contenidos de carbonato. *Revista Colombiana de Materiales. DOI:https://doi.org/10.17533/udea.rcm.n17a03 .URL:https://revistas.udea.edu.co/index.php/materiales/article/view/344920.*, 22-32. Query Date: June 2022.

Palanive, C., N. P., & Selvakumar, G. (2019). Morphological expedient flower like nanostructures WO3–TiO2 nanocomposite material and its multi applications. *OpenNano. DOI:https://doi.org/10.1016/j.onano.2018.11.002.URL:https://www.sciencedirect.com/science/article/pii/S2352952018300690.*, 1-21, 4, 100026. Query Date: June 2022.

Reyes, C. (2002). La Química Verde y la problemática de los residuos. *Ciencia en Desarrollo.URL:https://revistas.uptc.edu.co/index.php/ciencia_en_desarrollo/article/view/261*, 2(2), 131-146. Query Date: June 2022.

Rivera, R., Riaño, H., Echavarría, A., Monsalve, P., Alzate, G., Restrepo, L., & Jaramillo, C. (2004.). Injertos óseos - Nueva alternativa. Fase III.Obtención, caracterización y evaluación de Hidroxiapatita Sintética y el compuesto de Hidroxiapatita Sintética porosa – Proteínas Morfogenéticas Óseas en un modelo experimental Lapino. URL:https://www.redalyc.or. *Revista Colombiana de Ciencias Pecuarias*, 20-28. Query Date: June 2022.

Saravanakkumar, D., Oualid, H. A., Brahmic, Y., Ayeshamariam, A., Karunanaithy, A., Mohamed Saleeme, A., Kaviyarasu, K., Sivaranjanih, S., Jayachandran, M. (2019). Synthesis and characterization of CuO/ZnO/CNTs thin films on copper substrate and its photocatalytic applications.DOI:https://doi.org/10.1016/j.onano.2018.11.001. *OpenNano. URL: https://www.sciencedirect.com/science/article/pii/S2352952018300586.*, 1-15. Query Date: June 2022.

Timchenko, P. E., Timchenko, E. V., Frolov, O. O., Volova, L. T., & Pisareva, E. V. (2018). Detailed Analysis of Raman Spectra for Express Assessment of the Hydroxyapatite Quality. *IEEE International Conference on Electrical Engineering and Photonics. DOI:10.1109/EExPolytech.2018.8564425.URL: https://ieeexplore.ieee.org/document/8564425.*, 233-235. Query Date: June 2022.

Xiong, G., Pal, U., & García Serrano, J. (2007). Correlations among size, defects, and photoluminescence in ZnO nanoparticles. *Journal of Applied Physics. DOI: https://doi.org/10.1063/1.2424538.URL:http://www.ifuap.buap.mx/~upal/assets/110.pdf.*, *101*(2), 024317-1, 024317-6. Query Date: June 2022.

Yilmaz, B., & Elvis, Z. (2014). Raman Spectroscopy Investigation of Nano Hydroxyapatite Doped with Yttrium and Fluoride Ions. *Spectroscopy Letters.DOI: https://doi.org/10.1080/00387010.2013.778296 .URL:https://www.ingentaconnect.com/content/tandf/speclet/2014/00000047/00000001/art00005., 47*(1), 24-29. Query Date: June 2022.

ISSN: 2410-3934